Cellular and Molecular Biology
E-ISSN : 1165-158X / P-ISSN : 0145-5680
www.cellmolbiol.org

Original Research

Physicochemical and biological characterization of a xanthan gum-polyvinylpyrrolidone hydrogel obtained by gamma irradiation

Tania López-Huante[1], María L. Del Prado-Audelo[1,2*], Isaac H. Caballero-Florán[1,3], Octavio D. Reyes-Hernández[4], Gabriela Figueroa-González[5], Manuel González-Del Carmen[6], David M. Giraldo-Gomez[7,8], Javad Sharifi-Rad[9,10], Maykel González-Torres[11], Hernán Cortes[12], Gerardo Leyva-Gómez[1*]

[1] Departamento de Farmacia, Facultad de Química, Universidad Nacional Autónoma de México, Ciudad Universitaria, Circuito Exterior S/N, Del. Coyoacán, Ciudad de México 04510, Mexico
[2] Escuela de Ingeniería y Ciencias, Departamento de Bioingeniería, Tecnológico de Monterrey Campus Ciudad de México, Ciudad de México, 14380, Mexico
[3] Departamento de Fisiología, Biofísica & Neurociencias, Centro de Investigación y de Estudios Avanzados del Instituto Politécnico Nacional, Ciudad de México 07360, Mexico
[4] Laboratorio de Biología Molecular del Cáncer, UMIEZ, Facultad de Estudios Superiores Zaragoza, Universidad Nacional Autónoma de México, 09230, Mexico City, Mexico
[5] Laboratorio de Farmacogenética, UMIEZ, Facultad de Estudios Superiores Zaragoza, Universidad Nacional Autónoma de México, Ciudad de México 09230, Mexico
[6] Facultad de Medicina, Universidad Veracruzana, Ciudad Mendoza, 94740, Veracruz, Mexico
[7] Departamento de Biología Celular y Tisular, Facultad de Medicina, Universidad Nacional Autónoma de México, Ciudad de México, 04510, Mexico
[8] Unidad de Microscopía, Facultad de Medicina, Universidad Nacional Autónoma de México, Ciudad de México, 04510, Mexico
[9] Phytochemistry Research Center, Shahid Beheshti University of Medical Sciences, Tehran, Iran
[10] Facultad de Medicina, Universidad del Azuay, Cuenca, Ecuador
[11] CONACyT-Laboratorio de Biotecnología, Instituto Nacional de Rehabilitación Luis Guillermo Ibarra Ibarra, Ciudad de México, 14389, Mexico
[12] Laboratorio de Medicina Genómica, Departamento de Genómica, Instituto Nacional de Rehabilitación Luis Guillermo Ibarra Ibarra, Ciudad de México, 14389, Mexico

[*]**Correspondence to:** luisa.delpradoa@gmail.com; leyva@quimica.unam.mx

Received August 5, 2020; **Accepted** November 6, 2020; **Published** January 31, 2021
Doi: http://dx.doi.org/10.14715/cmb/2021.67.1.11

Abstract: Xanthan gum (XG) and polyvinylpyrrolidone (PVP) are two polymers with low toxicity, high biocompatibility, biodegradability, and high hydrophilicity, making them promising candidates for multiple medical aspects. The present work aimed to synthesize a hydrogel from a mixture of XG and PVP and crosslinked by gamma irradiation. We assessed the hydrogel through a series of physicochemical (FT-IR, TGA, SEM, and percentage of swelling) and biological (stability of the hydrogel in cell culture medium) methods that allowed to determine its applicability. The structural evaluation by infrared spectrum demonstrated that a crosslinked hydrogel was obtained from the combination of polymers. The calorimetric test and swelling percentage confirmed the formation of the bonds responsible for the crosslinked structure. The calorimetric test evidenced that the hydrogel was resistant to decomposition in contrast to non- irradiated material. The determination of the swelling degree showed constant behavior over time, indicating a structure resistant to hydrolysis. This phenomenon also occurred during the test of stability in a cell culture medium. Additionally, microscopic analysis of the sample revealed an amorphous matrix with the presence of porosity. Thus, the findings reveal the synthesis of a novel material that has desirable attributes for its potential application in pharmaceutical and biomedical areas.

Key words: Polyvinylpyrrolidone; Xanthan gum; Hydrogel; Gamma irradiation; Crosslinking.

Introduction

Hydrogels are insoluble three-dimensional networks formed from polymer chains capable of absorbing large quantities of water or biological fluids due to functional groups in their structure such as -OH-, -COOH, $-CONH_2$, and $-SO_3H$ (1–3). Their applications include the control of drug release (4) and tissue repair (5–7), which is part of tissue engineering, in which hydrogels function as scaffolding that provides a supporting structure for cell adhesion, migration, and proliferation (8). Likewise, resistance to mechanical forces, degradation stability, and chemical functionality (2) make chemical hydrogels candidates for biomedical applications. A wide variety of hydrogels have been developed and classified according to their origin, response to stimuli, or crosslinking (9,10). One of the advantages of chemical hydrogels is that their synthesis can be carried out by different methods (11,12), including the crosslinking by gamma radiation. This technique's principle is mainly

based on the use of a radioactive isotope (^{60}Co) as a medium for the formation of ionized molecules and free radicals (13). The relevance of this method lies in its low cost and elimination of the use of chemical crosslinkers; furthermore, it promotes a complete reaction between chemical species in the medium and provides a pure and sterile product (14–16). Among the materials with potential for hydrogels© synthesis, polymers of natural origin such as xanthan gum (XG) and synthetic origin such as polyvinylpyrrolidone (PVP) are included. XG is a natural polymer obtained by the fermentation of carbohydrates by bacteria of the genus Xanthomonas (17), it is biocompatible, hydrophilic and promotes cell adhesion, proliferation, and cell migration (18), furthermore is also suitable for modified drug release (19). In contrast, PVP is a synthetic polymer that has also shown potential application in the synthesis of hydrogels due to its biocompatibility, low toxicity, and the ability to generate porous structures (20,21).

Therefore, in this study, we synthesized a hydrogel from a natural polymer and one synthetic crosslinked with gamma rays. The hydrogel was physicochemically characterized by Fourier transform infrared spectroscopy (FT-IR), thermogravimetric analysis (TGA), and swelling degree. Moreover, we examined the morphology of the material with scanning electron microscopy (SEM). Finally, we performed a biological evaluation by determining the stability of the hydrogel in a cell medium. Due to the combined use of natural and synthetic polymers, it was expected to obtain a hydrogel with optimal biological and physicochemical characteristics for possible tissue engineering applications as a scaffold. Furthermore, the use of gamma radiation favors the generation of a sterile product free of chemical crosslinkers.

Materials and Methods

Materials

PVP K-30 (Kollidon® 30, Mw 8,000 Da) was obtained from BASF® (Germany). The XG was acquired from Disan® (Mexico). The Dulbecco's modified eagle medium: nutrient mixture F-12 (DMEM F/12), penicillin and Fetal bovine serum (FBS) were purchased from ThermoFisher® (Carlsbad, CA, USA).

Sample preparation

Preparation of the aqueous solution of XG and PVP (XG+PVP)

The hydrogel was prepared as follows: 36 g of PVP k-30 was added in 400 mL of distilled water and was stirred until its dissolution, soon after 4 g of XG was added to the same mixture, generating an aqueous solution in proportion 9:1. The solution was homogenized with a stirring rod at room temperature.

Preparation of irradiated hydrogel (XG-PVP)

The mixture of polymers in aqueous solution was exposed to gamma radiation with ^{60}Co as a source of irradiation, using a Gammabeam 651PT pool radiator and Fricke dosimeters dose 25 kGy.

Physicochemical characterization

A sample of the XG-PVP hydrogel was extracted and freeze-dried at -49°C, with a pressure of 0.05 mBar for 24 h. In order to evaluate the physicochemical properties, the lyophilized hydrogel was characterized by FT-IR, TGA, SEM, and its swelling degree was determined with the hydrogel without lyophilizing.

Fourier transform infrared spectroscopy

Samples of the lyophilized XG-PVP, the polymer mixture (XG+PVP), and the unit components (XG and PVP) were collected and analyzed with FT-IR to determine the possible formation of covalent bonds. The results were recorded in an FTIR Nicolet 6700 spectrophotometer in a range of 4000-500 cm^{-1}.

Thermogravimetric analysis

XG, PVP, XG+PVP, and XG-PVP were evaluated employing a Hi-Res TGA 2950 thermogravimetric equipment to know their thermal stability. Each sample was analyzed in an ambient temperature range to 500 °C, with a heating ramp of 10 °C/min, in a nitrogen atmosphere.

Swelling degree

Portions of approximately 1 g of XG+PVP (control sample) and XG-PVP were exposed to a medium containing distilled water. Each sample was weighed in falcon tubes after eliminating the excess of the medium every 24 h; five days were taken as the maximum time. This test was done by triplicate.

We calculated the swelling degree of control and the XG-PVP sample using equation 1, where m_f is the mass of swollen hydrogel and m_0 is the initial mass of hydrogel:

$$\% \text{ Swelling} = (m_f - m_0)/m_0 \times 100 \quad (1)$$

Scanning electron microscopy

We evaluated the morphology and pore size of XG-PVP by SEM in a field emission scanning electron microscope (Zeiss Crossbeam 550) with a focused ion beam (FIB-SEM). For the determination, the samples were coated with a thin layer of gold by plasma-assisted deposition using the JEOL Fine Coat Ion Sputter JFC-1100.

Biological characterization

We evaluated the stability of irradiated hydrogel in a cell culture medium. Samples of XG-PVP without lyophilizing were cut in thin layers and positioned in 200 µL of cell culture medium DMEM F/12/penicillin 1%/FBS 10% for a period of 96 h. Each layer was extracted from the medium every 24 h, and its physical changes were evaluated macroscopically.

Results

Physicochemical characterization

FT-IR

Figure 1 exposes the analysis of the functional groups of the samples employing the FT-IR. Infrared spectrum of XG (Figure 1a) demonstrated signals at 3336 cm^{-1} due to the O-H stretching of alcohol and carboxylic acid; a signal at 2910 cm^{-1} due to the stretching of C-H, possibly due to the absorption of symmetrical

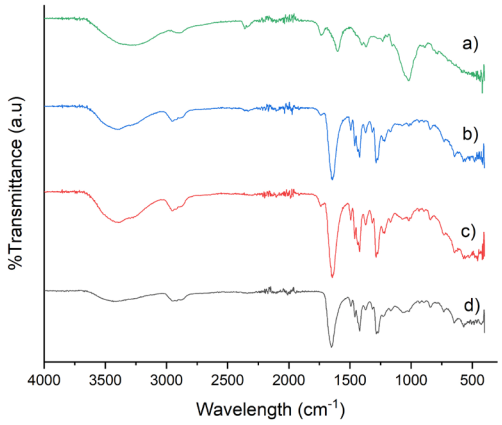

Figure 1. FT-IR spectra of pure components and hydrogels. a) XG, b) PVP, c) XG+PVP (control), and d) XG-PVP, respectively.

and asymmetric stretches of CH_3 or even groups of CH_2 and CHO (22); a signal at 1739 cm^{-1} due to the stretching of the C=O group of carboxylic acids or ester; and at 1031 cm^{-1} a signal of low-intensity possibly due to the C-O stretching. Concerning PVP (Figure 1b), a vibration C-H of the CH_2 was found at 2913 cm^{-1} and torsion of the same group at 1440 cm^{-1}; the vibration C-H by the group CH in 2885 cm^{-1}; the vibration of the groups C=O in 1646 cm^{-1}; and the stretching of C-N at 1280 cm^{-1} belonging to pyrrolidone and a low-intensity signal at 725 cm^{-1} by the interaction C-C (23). Meanwhile, the line corresponding to XG+PVP (Figure 1c) exhibited signals remarkably similar to those expressed by the PVP. In contrast, XG-PVP (Figure 1d) did not demonstrate the same behavior, as the signals present at 3399 cm^{-1}, 2950 cm^{-1}, 1214 cm^{-1}, and 736 cm^{-1} (present in the control hydrogel) corresponding to the stretching of O-H, CH_2, and the C-C interactions (respectively), were displaced and decreased in the irradiated sample. In XG-PVP, these signals were displayed in bands at 3417 cm^{-1}, 2944 cm^{-1}, 1220 cm^{-1}, and 730 cm^{-1}. Besides, a signal expressed in the control sample in the region near 1739 cm^{-1} disappeared. These results point out a possible structural change in the polymers present in the irradiated sample.

Thermogravimetric analysis

The thermal behavior of different samples was determined by TGA (Figure 2). We observed a weight loss at a temperature of approximately 265 °C for XG (Figure 2a) and 424 °C for PVP (Figure 2b); such losses corresponded to 45% and 86%, respectively. Likewise, two losses were denoted for XG+PVP (Figure 2c) at 269 °C (0.6%) and 420 °C (66.7%). In contrast, two signals at 281 °C and 435 °C on XG-PVP (Figure 2d) indicated decomposition of 7.4% and 66.4%, suggesting a change in its thermal profile.

Swelling behavior

The determination of the swelling behavior of the hydrogels (XG+PVP and XG-PVP) in a medium containing water is depicted in Figure 3. The comparison between XG+PVP (Figure 3a) and XG-PVP (Figure 3b) demonstrated a stable behavior of XG-PVP and an increase of 10-15% in the swelling degree.

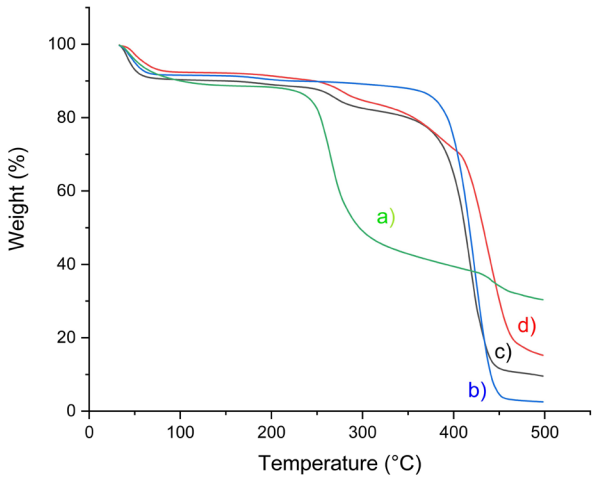

Figure 2. Thermogravimetric analysis. a) XG, b) PVP, c) XG+PVP (control), and d) XG-PVP, respectively.

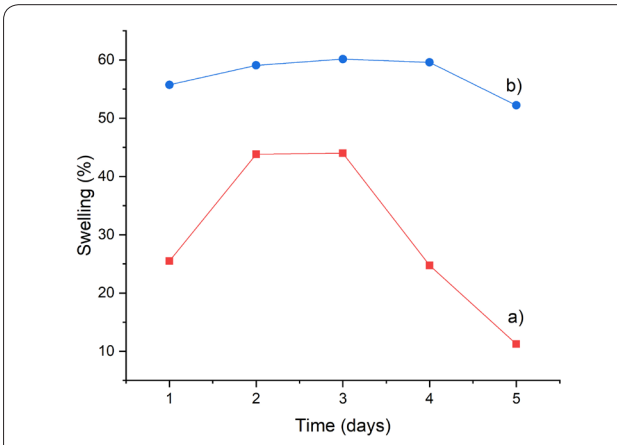

Figure 3. Swelling behavior in the water of hydrogels at room temperature. a) XG+PVP (control), and b) XG-PVP.

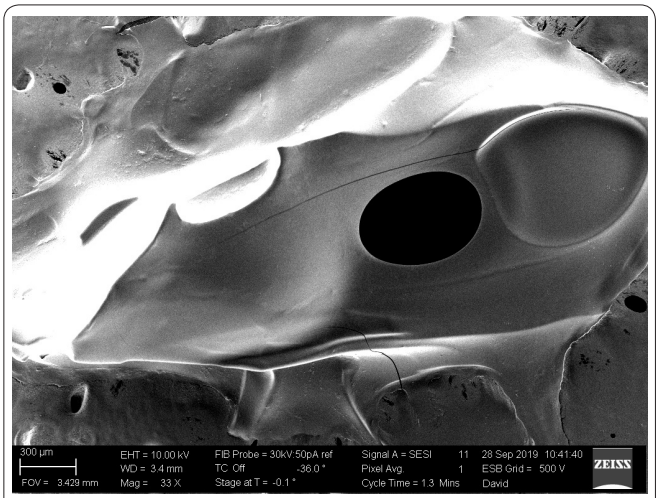

Figure 4. SEM image of the XG-PVP hydrogel produced by gamma irradiation.

Scanning electron microscopy

We accomplished the evaluation of the morphology and pore size of XG-PVP by SEM. The analysis performed in different areas of the material demonstrated an amorphous matrix with pores with a length of 300 µm (Figure 4).

Biological characterization

We evaluated the stability of PVP hydrogel in a cell culture medium to perform the biological characteriza-

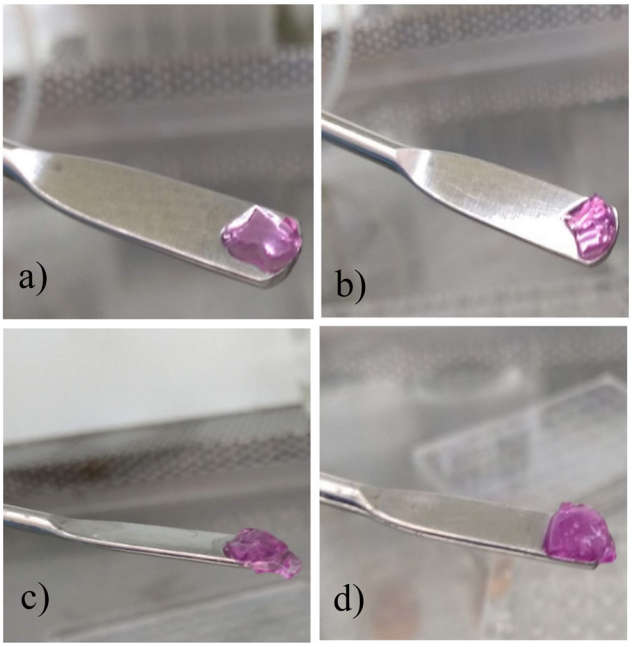

Figure 5. Stability of XG-PVP in cell culture medium at different contact times. a) 24 h, b) 48 h, c) 72 h, d) 96 h, respectively.

tion. Figure 5 shows the hydrogel's behavior when exposed to the cell culture medium. Periodic evaluation of the lamellae for four days revealed a gradual increase in the material's size due to its swelling. However, the macroscopic study determined the hydrogel's full conservation because we did not find signs of ruptures or degradation in the samples.

Discussion

XG and PVP (Figure 6) are non-toxic, biodegradable, biocompatible, and low-cost products (24). Additionally, XG exhibits pseudoplastic behavior, gelling capacity, and water retention (25). The importance of XG in the synthesis of hydrogels lies in its nature as a polysaccharide, which gives it biochemical similarities with the extracellular matrix (ECM) (26), allowing the fabrication of scaffolds suitable for cell development that can be used in tissue engineering (27–29). On the other hand, PVP has a broad application in the pharmaceutical industry; however, its application in biomedical fields is limited, primarily due to its differences concerning to body tissues. Due to their promising characteristics, we created a hydrogel combining these two polymers in an aqueous medium and exposed to a high-energy source of irradiation. Subsequently, we employed several methods for physicochemical and biological characterization of the new biomaterial.

First, we carried out a structural characterization by FT-IR to determine functional groups (Figure 1). In concordance with previous reports, we observed several characteristic bands corresponding to XG and PVP (30,31). However, during the determination of the spectrum corresponding to XG+PVP, we found signals at similar values to the PVP spectrum. This phenomenon may result from the predominance of the concentration of PVP regarding XG (9:1). Nevertheless, in the XG-PVP spectrum, we observed a shift of those signals and decreased intensity, suggesting new covalent bonds in the polymeric chains (32,33). Likewise, the signal's dis-

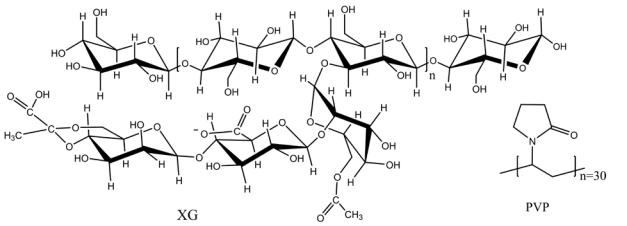

Figure 6. Structures of xanthan gum (XG) and polyvinylpyrrolidone (PVP).

appearance at 1739 cm^{-1} indicates a probable formation of hydrogen bonds between the two polymers. The appearance of these bonds is responsible for the production of a cross-network characteristic of hydrogels. It comes mainly from the generation of free radicals obtained by the incidence of gamma rays in the sample, which follow the chain reactions typical of radicals that, in addition to the initiation, include propagation and completion of the process (13). Besides the formation of polymer radicals, it has been demonstrated that hydroxyl radicals and hydrogen atoms are also present in the medium and come mainly from water radiolysis (34,35). The hydroxyl radicals transfer the water's reactivity to the polymer chains, since they extract the hydrogen atoms from the macromolecules, producing macroradicals that react to each other to create bonds (15).

In order to illustrate the synthesis of the XG-PVP cross-structure, we proposed a reaction mechanism that would indicate the possible binding sites between the two polymers (Figure 7). Here, HOOC-XG-OH is used to depict XG showing multiple hydroxyls (-OH) and carboxyl (-COOH) ends-groups. Initially, the hydroxyl radicals produced in spurs randomly deactivate radicals from the polymers. Simultaneously, the primary radicals of XG and PVP are formed. The XG carboxyl and all hydroxyl groups are susceptible to yield primary radicals. From PVP, the carbons marked as 6 and 7 are available to form primary radicals in the presence of gamma radiation. Next, the deactivation reaction of XG and PVP primary radicals is suggested. Therefore, PVP radicals can be grafted onto various positions in the polysaccharide. Also, the chain scission of the glycoside groups owed to radiolitic degradation has been reported for doses over five kGy (36,37). As a result, new hydroxyl groups will be available to react with the PVP primary radicals or water hydroxyl radicals.

Subsequently, we performed a TGA that allowed us to identify each of the sample's thermal behavior and corroborate the bond formation. The thermograph in Figure 2 displays the breakdown of raw materials and hydrogels (XG+PVP and XG-PVP). XG exhibited a loss of mass of 45% at a temperature of 265 °C (Figure 2a); according to data reported, this loss is attributed to the elimination of CO_2, pyruvate, and dimethyl group (38). Whereas PVP (Figure 2b) had a significant mass loss of 86% close to 424 °C, which may result from the release of CO_2 and pyrrolidone (39). Comparison of the results for raw materials (XG and PVP) and hydrogels (XG+PVP and XG-PVP) showed similar decomposition temperatures; therefore, it could be assumed that the values of 269 °C and 281 °C correspond to the decay of XG, while the values of 420 °C and 435 °C describe

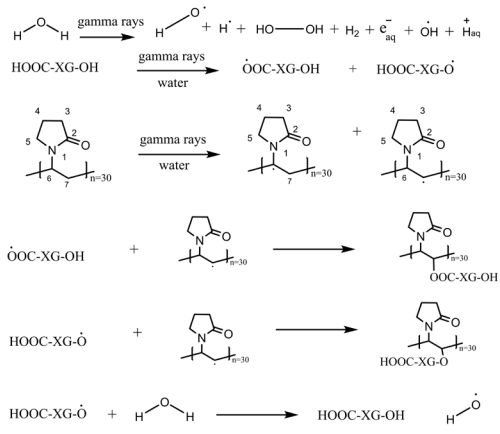

Figure 7. Proposed mechanism for the XG−PVP hydrogel synthesis.

the behavior of PVP. A notable difference between raw materials and hydrogels is exposed in the percentage of weight loss, as XG+PVP and XG-PVP samples presented a lower loss than PVP and XG, demonstrating the presence of interactions between the functional groups of the two polymers. Nonetheless, in XG+PVP, the decrease in weight loss would be attributed to the formation of hydrogen bonds between the polymer chains, while in the case of XG-PVP, it is due to a new structure composed mainly of covalent bonds. This hypothesis would be supported by the remaining weight present at the test end, since XG-PVP had a residual weight of almost 20%, while XG+PVP presented 10%. This finding is explained by the increased resistance of the irradiated material to degradation due to the new bonds formed by gamma irradiation.

Another method applied in the hydrogel study was determining the swelling behavior (Figure 3), which revealed the tendency of XG+PVP and XG-PVP when exposed to an aqueous medium at room temperature. The exposure of XG+PVP to the medium exposed a balance in the capacity of swelling after the first 48 h of the experiment, and it was that same time in which that behavior remained stable. This fact can be explained by the existence of weak interactions in polymer chains that breakthrough hydrolysis when coming into contact with water, which causes a gradual degradation of the material. In contrast, the XG-PVP exhibited an increase in swelling degree and a rapid balance in the swelling capacity that begins from the first moment of exposure to the medium and remains stable up to 96 h. Both characteristics in XG-PVP can be due to covalent bonds between the polymers that generate a crosslinked network and the XG's helical structure (24) that prevent degradation by hydrolysis. Also, crosslinking by gamma irradiation promotes the synthesis of a structure whose hydrophilic groups are more exposed and which, in contact with water, generate the expansion of the network (40). Swelling is one of the essential characteristics in hydrogels since specific pharmaceutical applications such as wound repair, require this aspect to absorb exudates generated in the affected site, whose removal helps heal (41).

On the other side, in biomedical applications, the generation of an expandable structure promotes the imitation of the ECM, and the water intake in the network supports the exchange of cells and nutrients. The morphology and characteristics of the material were obtained by an SEM analysis (Figure 4), indicating the existence of pores of 300 µm in an amorphous matrix, which could represent an advantage since porous structures allow the exchange of nutrients, cell ingrowth, and even angiogenesis (42). Several authors have reported distinct pore sizes suitable for different conditions: approximately 5 µm for neovascularization, 5-15 µm for internal fibroblast growth, 20 µm for hepatocyte growth, 20-125 µm for skin regeneration of adult mammals, and 200-350 µm for osteoconduction (10). Nonetheless, Cheng et al. (43) demonstrated that magnesium scaffolds with a pores size of 250-400 µm promote cell differentiation, and larger pores also lead to bone formation in the implant size. Therefore, our results would indicate an optimal pore size for hydrogels intended for biomedical scaffoldings. Besides, the presence of pores in the hydrogel makes it a candidate for the administration of drugs since it allows a controlled diffusion of its contents by allowing the entry of water (44).

Finally, to determine the hydrogel's stability in the culture medium, an experiment was conducted to evaluate the degradation of the product in the culture medium DMEM F/12/Penicillin 1%/FBS 10%. This test revealed an increase in the size of XG-PVP sheets after 24 h (Figure 5). The hydrogel's size remained constant along the days, without traces of degradation or rupture in the samples, indicating high stability of the hydrogel in the medium, which results from the formation of the cross-network between the polymers. This finding is relevant because a stable hydrogel in the medium would promote a desirable scaffold for tissue engineering. Eyrich et al. (45) demonstrated that long-term gels promote cartilaginous tissue development after contact with chondrocytes. Additionally, Trattnig et al. (46) performed the morphological evaluation of a commercial hydrogel that remained stable for months after implantation in the patient, providing a matrix able to stimulate cartilage regeneration.

In summary, we synthesized a hydrogel from a natural product combined with a synthetic polymer, which exhibited suitable morphology, stability, and crosslinking characteristics. Therefore, this new material could be considered for applications focused on the biomedical field.

In this work, we obtained an XG-PVP hydrogel using gamma radiation as a crosslinking agent of polymer chains. The choice of this synthesis method was largely based on that it is an economical and straightforward method, and sterile products are obtained. Our tests provided evidence on the synthesis of an interwoven polymer product with optimal characteristics such as suitable pore size, stability in the swelling process, and steadiness when exposed to a cellular environment. Moreover, the combination of polymers promises the generation of a material with high potential for pharmaceutical and biomedical applications as both materials are classified as biocompatible and biodegradable. Lastly, the use of a naturally occurring product such as XG would allow obtaining a hydrogel that could mimic the ECM.

Acknowledgments
This research was funded by CONACYT A1-S-15759 to Gerardo Leyva-Gómez. The authors thank Miguel Ángel Canseco-Martínez for the help of FTIR analysis, Karla Eriseth Reyes-Morales, for her technical assistance with thermal tests, Ana Bobadilla-Valencia for her technical aid with nitrogen handling used in the experimental setting. And to Elba Carrazco Ramirez, Irma Elena López Martínez, and Ivonne Grisel Sánchez Cervantes from the Microscopy Core Facility from the School of Medicine at the UNAM for their technical assistance with microscopy assessment.

Interest conflict
The authors declare no conflict of interest.

References

1. Peppas NA, Bures P, Leobandung W, Ichikawa H. Hydrogels in pharmaceutical formulations. Eur J Pharm Biopharm. 2000; 50:27–46.
2. Parhi R. Cross-linked hydrogel for pharmaceutical applications: A review. Adv Pharm Bull. 2017; 7:515–30.
3. Mishra B, Upadhyay M, Reddy Adena S, Vascant B, Muthu M. Hydrogels: An Introduction to a Controlled Drug Delivery Device, Synthesis and Application in Drug Delivery and Tissue Engineering. Austin J Biomed Eng. 2017; 4:1037–1.
4. Li J, Mooney DJ. Designing hydrogels for controlled drug delivery. Nat Rev Mater. 2016; 1: 16071.
5. Yuan F, Ma M, Lu L, Pan Z, Zhou W, Cai J, et al. Preparation and properties of polyvinyl alcohol (PVA) and hydroxylapatite (HA) hydrogels for cartilage tissue engineering. Cell Mol Biol (Noisy-le-grand). 2017; 63:32–5.
6. Aswathy SH, Narendrakumar U, Manjubala I. Commercial hydrogels for biomedical applications. Heliyon. 2020; 6:e03719.
7. Leyva-Gómez G, Santillan-Reyes E, Lima E, Madrid-Martínez A, Krötzsch E, Quintanar-Guerrero D, et al. A novel hydrogel of poloxamer 407 and chitosan obtained by gamma irradiation exhibits physicochemical properties for wound management. Mater Sci Eng C. 2017; 74:36–46.
8. Peppas NA, Hilt JZ, Khademhosseini A, Langer R. Hydrogels in biology and medicine: From molecular principles to bionanotechnology. Adv Mater. 2006; 18:1345–60.
9. Ahmed EM. Hydrogel: Preparation, characterization, and applications: A review. J Adv Res. 2015; 6:105–21.
10.El-Sherbiny IM, Yacoub MH. Hydrogel scaffolds for tissue engineering: Progress and challenges. Glob Cardiol Sci Pract. 2013; 2013:38.
11.Hunt JA, Chen R, Van Veen T, Bryan N. Hydrogels for tissue engineering and regenerative medicine. J Mater Chem B. 2014; 2:5319–38.
12.Zhang YS, Khademhosseini A. Advances in engineering hydrogels. Science. 2017; 356: eaaf3627.
13.Makuuchi K, Cheng S. Radiation Processing of Polymer Materials and its Industrial Applications. Radiation Processing of Polymer Materials and its Industrial Applications. John Wiley & Sons, New York, 2011, pp 15-16.
14.Muñoz-Muñoz F, Bucio E. Functionalization with Interpenetrating Smart Polymer Networks by Gamma Irradiation for Loading and Delivery of Drugs. In: Responsive Materials and Methods. Hoboken, NJ, USA: John Wiley & Sons, Inc.; 2013. p. 59–104.
15.Rosiak JM, Ulański P. Synthesis of hydrogels by irradiation of polymers in aqueous solution. Radiat Phys Chem. 1999; 55:139–51.
16.Mantha S, Pillai S, Khayambashi P, Upadhyay A, Zhang Y, Tao O, et al. Smart hydrogels in tissue engineering and regenerative medicine. Materials (Basel). 2019; 12:3323.
17.Petri DFS. Xanthan gum: A versatile biopolymer for biomedical and technological applications. J Appl Polym Sci. 2015; 132:42035.
18.Alves A, Miguel SP, Araujo ARTS, Jes D. Xanthan Gum – Konjac Glucomannan Blend Hydrogel. Polymers (Basel). 2020; 12:1–15.
19.Cortes H, Caballero-Florán IH, Mendoza-Muñoz N, Escutia-Guadarrama L, Figueroa-González G, Reyes-Hernández OD, et al. Xanthan gum in drug release. Cell Mol Biol (Noisy-le-grand). 2020 Jun 25; 66:199–207.
20.Román-Doval R, Tellez-Cruz MM, Rojas-Chávez H, Cruz-Martínez H, Carrasco-Torres G, Vásquez-Garzón VR. Enhancing electrospun scaffolds of PVP with polypyrrole/iodine for tissue engineering of skin regeneration by coating via a plasma process. J Mater Sci. 2019; 54:3342–53.
21.Jeong J-O, Park J-S, Kim Y-A, Yang S-J, Jeong S-I, Lee J-Y, et al. Gamma Ray-Induced Polymerization and Cross-Linking for Optimization of PPy/PVP Hydrogel as Biomaterial. Polymers (Basel). 2020; 12:111.
22.Faria S, De Oliveira Petkowicz CL, De Morais SAL, Terrones MGH, De Resende MM, De Frana FP, et al. Characterization of xanthan gum produced from sugar cane broth. Carbohydr Polym. 2011; 86:469–76.
23.Basha MAF. Magnetic and optical studies on polyvinylpyrrolidone thin films doped with rare earth metal salts. Polym J. 2010; 42:728–34.
24.Elella MHA, Mohamed RR, ElHafeez EA, Sabaa MW. Synthesis of novel biodegradable antibacterial grafted xanthan gum. Carbohydr Polym. 2017; 173:305–11.
25.Kim J, Hwang J, Seo Y, Jo Y, Son J, Choi J. Engineered chitosan–xanthan gum biopolymers effectively adhere to cells and readily release incorporated antiseptic molecules in a sustained manner. J Ind Eng Chem. 2017; 46:68–79.
26.Westin CB, Nagahara MHT, Decarli MC, Kelly DJ, Moraes ÂM. Development and characterization of carbohydrate-based thermosensitive hydrogels for cartilage tissue engineering. Eur Polym J. 2020; 129:109637.
27.Bellini MZ, Caliari-Oliveira C, Mizukami A, Swiech K, Covas DT, Donadi EA, et al. Combining xanthan and chitosan membranes to multipotent mesenchymal stromal cells as bioactive dressings for dermo-epidermal wounds. J Biomater Appl. 2015; 29:1155–66.
28.Juris S, Mueller A, Smith B, Johnston S, Walker R, Kross R. Biodegradable Polysaccharide Gels for Skin Scaffolds. J Biomater Nanobiotechnol. 2011; 02:216–25.
29.Kumar A, Rao KM, Han SS. Application of xanthan gum as polysaccharide in tissue engineering: A review. Carbohydr Polym. 2018; 180:128–44.
30.Nejadmansouri M, Shad E, Razmjooei M, Safdarianghomsheh R, Delvigne F, Khalesi M. Production of xanthan gum using immobilized Xanthomonas campestris cells: Effects of support type. Biochem Eng J. 2020; 157:1-13.
31.Roy N, Saha N, Kitano T, Saha P. Novel hydrogels of PVP-CMC and their swelling effect on viscoelastic properties. J Appl Polym Sci. 2010; 117:1703-1710.
32.Kumar A, Deepak, Sharma S, Srivastava A, Kumar R. Synthesis of xanthan gum graft copolymer and its application for controlled release of highly water soluble Levofloxacin drug in aqueous medium. Carbohydr Polym. 2017; 171:211–9.
33.Ochoa-Segundo EI, González-Torres M, Cabrera-Wrooman A, Sánchez-Sánchez R, Huerta-Martínez BM, Melgarejo-Ramírez Y, et al. Gamma radiation-induced grafting of n-hydroxyethyl acrylamide onto poly(3-hydroxybutyrate): A companion study on its polyurethane scaffolds meant for potential skin tissue engineering applications. Mater Sci Eng C. 2020; 116:111176.

34.González Torres M, Cerna Cortez J, Balam Muñoz Soto R, Ríos Perez A, Pfeiffer H, Leyva Gómez G, et al. Synthesis of gamma radiation-induced PEGylated cisplatin for cancer treatment. RSC Adv. 2018; 8:34718–25.
35.González-Torres M, Leyva-Gómez G, Rivera M, Krötzsch E, Rodríguez-Talavera R, Rivera AL, et al. Biological activity of radiation-induced collagen–polyvinylpyrrolidone–PEG hydrogels. Mater Lett. 2018; 214:224–7.
36.Hayrabolulu H, Demeter M, Cutrubinis M, Güven O, Şen M. Radiation induced degradation of xanthan gum in aqueous solution. Radiat Phys Chem. 2018; 144:189–93.
37.Fei B, Wach RA, Mitomo H, Yoshii F, Kume T. Hydrogel of biodegradable cellulose derivatives. I. Radiation-induced crosslinking of CMC. J Appl Polym Sci. 2000; 78:278–83.
38.Kang M, Oderinde O, Liu S, Huang Q, Ma W, Yao F, et al. Characterization of Xanthan gum-based hydrogel with Fe3+ ions coordination and its reversible sol-gel conversion. Carbohydr Polym. 2019; 203:139–47.
39.Bogatyrev VM, Borisenko NV, Pokrovskii VA. Thermal degradation of polyvinylpyrrolidone on the surface of pyrogenic silica. Russ J Appl Chem. 2001; 74:839–44.
40.Janićijević Ž, Vujčić I, Veljović Đ, Vujisić M, Radovanović F. Composite poly(DL-lactide-co-glycolide)/poly(acrylic acid) hydrogels synthesized using UV and gamma irradiation: comparison of material properties. Radiat Phys Chem. 2020; 166:108466.
41.Demeter M, Meltzer V, Călina I, Scărișoreanu A, Micutz M, Albu Kaya MG. Highly elastic superabsorbent collagen/PVP/PAA/PEO hydrogels crosslinked via e-beam radiation. Radiat Phys Chem. 2020; 174:108898.
42.Annabi N, Nichol JW, Zhong X, Ji C, Koshy S, Khademhosseini A, et al. Controlling the porosity and microarchitecture of hydrogels for tissue engineering. Tissue Eng - Part B Rev. 2010; 16:371–83.
43.Cheng MQ, Wahafu T, Jiang GF, Liu W, Qiao YQ, Peng XC, et al. A novel open-porous magnesium scaffold with controllable microstructures and properties for bone regeneration. Sci Rep. 2016; 6:1–14.
44.Caló E, Khutoryanskiy V V. Biomedical applications of hydrogels: A review of patents and commercial products. Eur Polym J. 2015; 65:252–67.
45.Eyrich D, Brandl F, Appel B, Wiese H, Maier G, Wenzel M, et al. Long-term stable fibrin gels for cartilage engineering. Biomaterials. 2007; 28:55–65.
46.Trattnig S, Ohel K, Mlynarik V, Juras V, Zbyn S, Korner A. Morphological and compositional monitoring of a new cell-free cartilage repair hydrogel technology - GelrinC by MR using semi-quantitative MOCART scoring and quantitative T2 index and new zonal T2 index calculation. Osteoarthr Cartil. 2015; 23:2224–32.